Recovery of ammonia from scrubber effluents using bipolar membrane electrodialysis
Assessing the effects of ammonium citrate - sulfate mixtures

Narayen, Dhavissen; Başli, Elif; Lier, Jules B.van; Spanjers, Henri

DOI
10.1016/j.desal.2025.119723

Publication date
2025

Document Version
Final published version

Published in
Desalination

Citation (APA)
Narayen, D., Başli, E., Lier, J. B. V., & Spanjers, H. (2025). Recovery of ammonia from scrubber effluents using bipolar membrane electrodialysis: Assessing the effects of ammonium citrate - sulfate mixtures. *Desalination*, *621*, Article 119723. https://doi.org/10.1016/j.desal.2025.119723

Desalination 621 (2026) 119723

Contents lists available at ScienceDirect

Desalination

journal homepage: www.elsevier.com/locate/desal

Recovery of ammonia from scrubber effluents using bipolar membrane electrodialysis: Assessing the effects of ammonium citrate - sulfate mixtures

Dhavissen Narayen [a,*], Elif Başli [a], Jules B.van Lier [a], Henri Spanjers [a]

[a] *Department of Water Management, Faculty of Civil engineering and Geosciences, Delft Delft University of Technology, Stevinweg 1, 2628 CN, Delft, the Netherlands*

HIGHLIGHTS

- Recovery of NH_3 from scrubber effluent by bipolar membrane electrodialysis (BPMED)
- Effect of NH_4^+ salts mixtures on energy use, NH_4^+ recovery and current efficiency
- Lower energy use with increasing ammonium citrate proportion
- Higher NH_4^+ recovery and current efficiency with increasing ammonium citrate proportion
- Assessment of NH_3 diffusion, H^+ and OH^- leakage at different NH_4^+ salts mixtures

ARTICLE INFO

Keywords:
Bipolar membrane electrodialysis
Ammonium recovery efficiency
Ammonium salt mixtures
Energy consumption
Current efficiency
Ammonia diffusion

ABSTRACT

Recent research showed that the recovery of ammonia from simulated ammonium citrate scrubber effluent via bipolar membrane electrodialysis (BPMED) is less energy-intensive than from ammonium sulfate solutions. Nonetheless, the application of citric acid as scrubbing agent is limited by its high costs. This study aimed to improve BPMED performance for ammonium recovery using ammonium salts mixtures (ammonium sulfate and ammonium citrate) as feed solutions. Unlike previous studies that focused mainly on single-salt systems, it investigated how this combination affects ammonium recovery efficiency, current efficiency, energy consumption, ammonia diffusion, H^+ and OH^- leakage to the diluate compartment, and anions transport across anion exchange membranes (AEMs) during BPMED. The ammonium recovery efficiency was higher for pure ammonium citrate (45.2 %) and mixture solutions (32.0–45.9 %) than for pure ammonium sulfate (26.8 %). Higher efficiency resulted from reduced competition between protons and ammonium across the cation exchange membrane (CEM). Feed with a higher ammonium citrate proportion increased buffer capacity, preventing protons leakage from the acid to the diluate compartment. This resulted in higher ammonium current efficiency for pure ammonium citrate (34.8 %) and mixture solutions (24.9–35.7 %) than for pure ammonium sulfate (20.4 %). The energy consumption was lower for pure ammonium citrate (14.1 kWh/kg-N recovered) and mixture solutions (13.0–17.4 kWh/kg-N recovered), than for pure ammonium sulfate (22.3 kWh/kg-N recovered). Ammonia diffusion from the base to the acid compartment reduced current efficiency by 19–23 % and accounted for 30–40 % of the total ammonium transported from the feed. This study demonstrated the effective use of ammonium citrate as one of the salts in the mixture to achieve high ammonium recovery efficiency with reduced energy consumption.

1. Introduction

Bipolar membrane electrodialysis (BPMED) is an electrochemical membrane technology that removes ions from a feed solution and simultaneously produces an acid and a base [1]. A BPMED stack consists of bipolar membranes (BPMs), anion-exchange membranes (AEMs), and cation-exchange membranes (CEMs). BPMs dissociate water into hydroxyl ions (OH^-) and protons (H^+), when an electric field is applied across them [2]. AEMs and CEMs enable the transfer of anions and cations from the feed compartment into the acid and base

---

* Corresponding author.

E-mail addresses: D.Narayen@tudelft.nl (D. Narayen), elifbasli13@gmail.com (E. Başli), j.b.vanlier@tudelft.nl (J.B.van Lier), h.l.f.m.spanjers@tudelft.nl (H. Spanjers).

https://doi.org/10.1016/j.desal.2025.119723
Received 16 October 2025; Received in revised form 30 November 2025; Accepted 1 December 2025

compartments, respectively. The anions combine with H^+ in the acid compartment forming the acid, while the cations combine with OH^- in the base compartment forming the base.

BPMED can be used to recover ammonia (NH_3) from ammonium (NH_4^+)-rich waters, such as reject waters from sludge dewatering units and ammonium scrubber effluents [3–12]. Although NH_4^+ in scrubber effluents can be recovered as dissolved NH_3 by the BPMED process without using chemicals [10], achieving a high NH_4^+ recovery efficiency at low electrochemical energy consumption remains a key challenge. During the batch-wise recovery process, the NH_4^+ recovery efficiency decreases as the NH_3 concentration in the base increases [13]. The main processes limiting the NH_3 recovery, among others, are NH_3 diffusion from the base to the acid compartment, or from the base to the diluate compartment, water diffusion from the diluate to the base compartment at high concentration gradients, and competitive H^+ transport across the CEM [10,12,13]– [15]. Li et al. [8] suggested increasing the current density to enhance NH_4^+ recovery efficiency in the base compartment. In addition, higher pH and lower temperature of scrubber effluents have been reported to improve NH_3 recovery [10]. Mutahi et al. [16] showed that BPMED with simulated ammonium citrate ($(NH_4)_3C_6H_5O_7$) effluent yielded higher NH_4^+ recovery and current efficiencies and lower energy consumption than ammonium sulfate ($(NH_4)_2SO_4$) solutions. However, the practical application of citric acid as a scrubbing agent is limited by its high cost [17].

In light of this, although ammonia recovery from scrubber effluents is well-established [10,16], simultaneous recovery of both dissolved NH_3 and acid by BPMED provides additional economic and operational benefits [10]. The recovered acid can be reused in the scrubbing process, reducing the need for additional chemicals, while the dissolved NH_3 serves as a valuable by-product for e.g. fertilizer production [10] or local energy supply [18]. This dual recovery lowers operational costs and enhances overall process sustainability. Therefore, optimizing base recovery at minimal energy consumption is particularly important when high-value acid recycling is also pursued. Despite these advantages, not all BPMED studies have focused on maximizing ammonium recovery.

In contrast, Wang et al. [19] focused on enhancing the acid rather than the base recovery efficiency, by using feed solutions with fixed sodium sulfate (Na_2SO_4) and varying $(NH_4)_2SO_4$ concentrations, with SO_4^{2-} as the common anion. Thus, the mixture of Na_2SO_4 and $(NH_4)_2SO_4$ had a higher salt concentration than a solution containing only Na_2SO_4 and this resulted in an enhancement of the migration of ions driven by the electric field [14,19,20]. Because of an increased electrical conductivity the stack resistance reduced and, therefore, the energy consumption for the BPMED process decreased [19]. However, in these studies ammonium was not considered as the common key-ion.

To our knowledge, no studies have evaluated BPMED performance for mixed ammonium salt solutions at a fixed NH_4^+ concentration, considering NH_4^+ recovery efficiency, NH_4^+ current efficiency, energy consumption, and NH_3 diffusion from the base to the acid compartment. This knowledge gap highlights the need to investigate the performance and feasibility of BPMED for treating mixed ammonium citrate - ammonium sulfate solutions, which could enable more cost-effective and sustainable ammonia recovery technologies.

Therefore, this study aims to assess the effect of different ammonium citrate and ammonium sulfate mixtures on the NH_4^+ recovery efficiency, NH_4^+ current efficiency, energy consumption, and NH_3 diffusion from the base to the acid compartment, using lab-scale BPMED experiments with simulated scrubber effluents. Additionally, this study also aims to assess the H^+ leakage from the acid to the diluate compartment, OH^- leakage from the base to the diluate compartment and anions transport across AEMs. We hypothesized that increasing the citrate content in mixed ammonium salt feeds will enhance BPMED performance by improving NH_4^+ recovery and current efficiency, lowering energy consumption through improved ion transport, reducing NH_3 diffusion from the base to the acid compartment, and mitigating H^+ accumulation in the diluate due to citrate's buffering capacity.

2. Materials and methods

2.1. Materials

The materials and the complete lab-scale BPMED set-up were similar to those previously described [10]. A BPMED membrane stack composed of ten repeating cell triplets was used, each forming a three-compartment cell configuration. Each cell triplet consisted of a PC 400D anion exchange membrane (AEM), a PC-SK cation exchange membrane (CEM) and a PC Bip bipolar membrane (BPM), all purchased from PCCell (Heusweiler, Germany). Key properties of the ion exchange membranes are provided in Table 1. PC 400D anion exchange end membranes (AEEMs), also supplied by PCCell (Heusweiler, Germany), were selected instead of cation exchange end membranes (CEEMs) to minimize NH_4^+ accumulation in the electrode rinse solution (ERS), while retaining Na^+ within the ERS. A schematic of the three-compartment BPMED membrane stack used in the experiments is shown in Fig. 1. All reagents, including ammonium citrate (≥ 97 %), were purchased from Sigma Aldrich (Zwijndrecht, The Netherlands).

2.2. Experimental methods

Lab-scale experiments were conducted to investigate the effects of NH_4^+ salt mixtures on the BPMED performance. The concentrations of $(NH_4)_2SO_4$ and $(NH_4)_3C_6H_5O_7$ in the feed solutions were varied according to Table 2, while the total initial NH_4^+ concentration was kept constant at 13.6 ± 0.1 g NH_4^+/L in all experiments, consistent with our previous work [10]. Each experiment was conducted for a duration of 135 min at a temperature of 25 ± 2 °C and an initial feed pH of 7.3 ± 0.1, adjusted using NH_4OH (25 %). Each experiment was conducted at an applied current density of 187.5 A/m^2, corresponding to the limiting current density (LCD) associated with 90 % NH_4^+ removal. The initial acid and base solutions each contained 0.5 L of demi water, with the initial pH and conductivity measured prior to each experiment but not adjusted. The preparation and concentration of the ERS followed the setup previously described [10]. The current, electric potential, pH and electrical conductivity (EC) of the solutions were recorded as previously described [10]. The solutions were sampled (sample volume = 2 mL) at the beginning, every 15 min, and at the end of each experiment to determine the NH_4^+, SO_4^{2-} and $C_6H_5O_7^{3-}$ concentrations. In addition, solution volumes were measured at the beginning and end of each experiment to assess the NH_4^+, SO_4^{2-} and $C_6H_5O_7^{3-}$ mass balances.

2.3. Analytical methods

The analytical methods used for the lab-scale BPMED experiments were similar to those previously described [10]. In addition, the $C_6H_5O_7^{3-}$ concentration was measured using a Metrohm 818 anion system Ion Chromatography (IC) with an A Supp 5150/4.0 anion column.

2.4. Performance indicators

The performance of the BPMED for the recovery of ammonia from ammonium salts mixture scrubber effluents was determined based on NH_4^+ recovery efficiency, NH_4^+ current efficiency, and energy consumption.

The NH_4^+ recovery efficiency was calculated as the ratio of the mass of ammonium recovered in the base to the mass of ammonium in the initial feed, as shown in eq. (1).

$$R_{NH_4^+}(t) = \frac{m_{NH_{4,b}^+}(t) - m_{NH_{4,b_i}^+}}{m_{NH_{4,f_i}^+}}.100\% \tag{1}$$

where $R_{NH_4^+}(t)$ = NH_4^+ recovery efficiency at time t (unit: %), $m_{NH_{4,b}^+}(t)$ = mass of NH_4^+ recovered in the base after time t (unit: g-NH_4^+), m_{NH_{4,b_i}^+} =

Table 1
Key properties of the ion exchange membranes utilized in the experiments, supplied by PCCell (Heusweiler, Germany).

Membrane	Thickness (μm)	Area resistance (Ω cm^2)	Water content (wt%)	Ion exchange capacity (meq.g^{-1})		Transport number (–)
				Strong basic	Weak basic	
AEM (PC 400D)	160–200	~ 10	~ 48	~ 0.66	~ 0.35	>0.86
CEM (PC-SK)	100–120	~ 2.5	~ 9	–		>0.95
BPM (PC Bip)	~ 120	–	~ 30	–		–

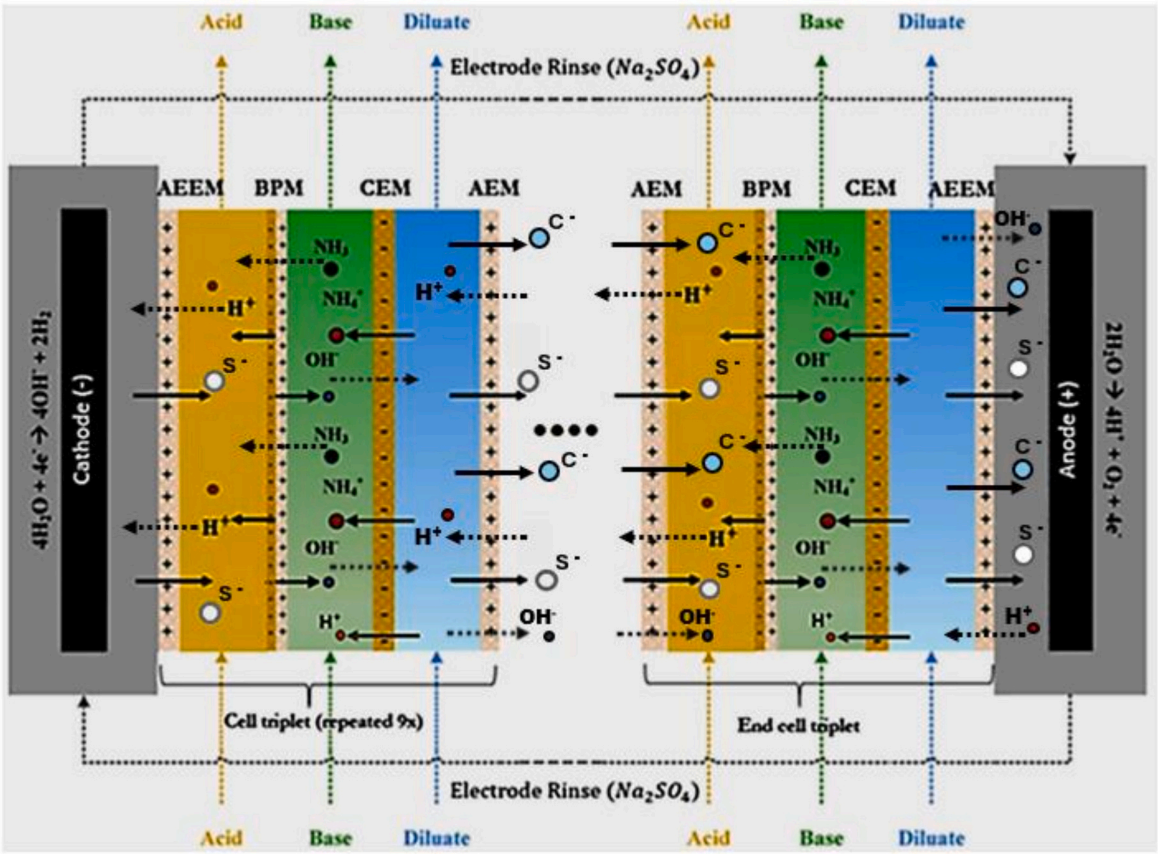

Fig. 1. Schematic representation of the three-compartment BPMED cell configuration and ion transport under an applied electric current. Various simulated scrubber effluents were fed into the feed /diluate compartment. In the acid compartment, H^+ combines with SO_4^{2-} (represented as S^-) and $C_6H_5O_7^{3-}$ (represented as C^-) to form a mixture of H_2SO_4 and citric acid ($C_6H_8O_7$), while in the base compartment, OH^- combines with NH_4^+ to form NH_4OH. The base compartment becomes rich in NH_3(aq) due to the high pH. Also shown are the undesired electromigration of citrate and sulfate ions toward the ERS, the electromigration of sulfate from the concentrated ERS to the acid compartment, and the undesired transport mechanisms (indicated by dotted arrows), including NH_3 diffusion from the base to the acid compartment, H^+ leakage from the acid to the diluate, and OH^- leakage through the CEM. The figure is adapted from van Linden et al. [12].

Table 2
Different feed solution mixtures with varying ammonium sulfate (AS) - ammonium citrate (AC) proportion, while maintaining a constant initial ammonium concentration of 0.757 ± 0.005 mol/L (13.6 ± 0.1 g NH_4^+/L).

SET NO	1	2	3	4	5	6	7	8	9
Proportion of AS and AC	AS100 - AC0	AS87.5 - AC12.5	AS75 - AC25	AS62.5 - AC37.5	AS50 - AC50	AS37.5 - AC62.5	AS25 - AC75	AS12.5 - AC87.5	AS0 - AC100
AS (mol/L)	0.378	0.331	0.284	0.236	0.189	0.142	0.095	0.047	0.000
AC (mol/L)	0.000	0.032	0.063	0.095	0.126	0.158	0.189	0.221	0.252
Ammonium (mol/L)	0.757	0.757	0.757	0.757	0.757	0.757	0.757	0.757	0.757
Sulphate (mol/L)	0.378	0.331	0.284	0.236	0.189	0.142	0.095	0.047	0.000
Citrate (mol/L)	0.000	0.032	0.063	0.095	0.126	0.158	0.189	0.221	0.252

initial mass of NH_4^+ in the base (unit: g-NH_4^+), $m_{NH^+_{4,f_i}}$ = initial mass of NH_4^+ in the feed (unit: g-NH_4^+).

The NH_4^+ current efficiency was calculated based on the recovered NH_4^+ using eq. (2).

$$\eta_{NH4^+}(t) = \frac{Z \cdot F \cdot n_{NH^+_{4,b}}(t)}{N \cdot \sum_{t=0}^{t} (I_t \cdot \Delta t)} \cdot \ 100\%, \tag{2}$$

where $\eta_{NH4+}(t)$ = NH_4^+ current efficiency at time t (unitless), z = ion valence (unitless, z = 1 for NH_4^+), F = Faraday constant (F = 96,485C. mol^{-1}), $n_{NH_{4,b}^+}(t)$ = amount of NH_4^+ recovered in the base after time t (unit: mol), N = number of cell triplets in the BPMED membrane stack (unitless, $N = 10$), I_t = electric current (unit: A), Δt = time interval (unit: s).

The energy consumption for NH_4^+ recovery from ammonium salts mixture scrubber effluents by BPMED was calculated using eq. (3).

$$E\ (t) = \frac{\sum_{t=0}^{t} (U_t \cdot I_t \cdot \Delta t) \cdot 18}{m_{NH_{4,b}^+}(t)\ \cdot 3600 \cdot 14}, \tag{3}$$

where E(t) = energy consumption at time t (unit: kWh/kg-N recovered), U_t = electric potential (unit: V).

Moreover, the distributions of NH_4^+ across the diluate, acid, and base compartments were determined to evaluate the NH_4^+ transport from the diluate to the base, as well as the NH_3 diffusion and NH_4^+ leakage from the base to the acid compartment through the BPM or from the base to the diluate compartment through the CEM [1,12]. The final fraction of NH_4^+ in the three compartments was calculated using the following Eq. [10]:

$$F_{NH_4^+}(t) = \frac{m_{NH_{4,s}^+}(t)}{m_{NH_{4,f_i}^+}} \cdot\ 100\%, \tag{4}$$

where $F_{NH_4^+}(t)$ = Final fraction of NH_4^+ at time t (unit: %),

$m_{NH_{4,s}^+}(t)$ = mass of NH_4^+ in respective compartment at time t (unit: g-NH_4^+).

To evaluate the anions transport through the AEMs, the anions (sulfate and citrate) removal efficiency was calculated as the ratio of the mass of anions removed from the diluate to the mass of anions in the initial feed, as shown in eq. (5).

$$r_{A^-}(t) = \frac{m_{A^-,f_i} - m_{A^-,d}(t)}{m_{A^-,f_i}} . 100\%, \tag{5}$$

where $r_{A^-}(t)$ = anions removal efficiency at time t (unit: %), m_{A^-,f_i} = initial mass of anions in the feed (unit: g), $m_{A^-,d}(t)$ = mass of anions in the diluate at time t (unit: g).

Furthermore, the anions (sulfate and citrate) mass balance across the diluate, acid, and base compartments were calculated as shown in eq. (6).

$$M_{A^-}(t) = \left(m_{A^-,d}(t) + m_{A^-,a}(t) + m_{A^-,b}(t)\right) - \left(m_{A^-,f_i} + m_{A^-,a_i} + m_{A^-,b_i}\right), \tag{6}$$

where $M_{A^-}(t)$ = anions mass balance across the diluate, acid, and base compartments at time t (unit: g), $m_{A^-,a}(t)$ = mass of anions in the acid at time t (unit: g), $m_{A^-,b}(t)$ = mass of anions in the base at time t (unit: g), m_{A^-,a_i} = initial mass of anions in the acid (unit: g), m_{A^-,b_i} = initial mass of anions in the base (unit: g).

The ion mobility in water, reflecting its movement through the solution, was calculated using the Einstein relation, as shown in eq. (7) [21,22].

$$u = \frac{DzF}{RT} \tag{7}$$

where u = mobility of the ion (unit: $m^2.V^{-1}.s^{-1}$), D = diffusion coefficient (m^2/s), z = ion valence (unitless, z = 1 for dihydrogen citrate (H_2Cit^-), z = 2 for hydrogen citrate ($HCit^{2-}$) and SO_4^{2-} and z = 3 for citrate (Cit^{3-})), R = ideal gas constant (R = 8.3145 J·K^{-1}·mol^{-1}), T = temperature (unit: K).

3. Results

3.1. Final NH_4^+ distribution and NH_4^+ recovery efficiency

The final NH_4^+ distribution across the diluate, acid, and base compartments reflected the net NH_4^+ transport, including NH_3 diffusion to the acid after an experimental run of 135 min with different feed mixtures of ammonium sulfate (AS) and ammonium citrate (AC) (Fig. 2A). Feed of 100 % AS (pure AS) compared to 100 % AC (pure AC) resulted in a lower mass of NH_4^+ recovered in the base at the end of the experimental run: 3.7 compared to 6.3 g-NH_4^+, respectively. Consequently, the mass of NH_4^+ retained in the diluate was higher for 100 % AS than for 100 % AC: 5.2 g-NH_4^+ compared to 2.2 g-NH_4^+ The difference in NH_4^+ mass recovered in the base between consecutive experimental runs decreased significantly as the proportion of AC in the feed increased from 0 % to 100 %. A comparison between the feed having 0 % AC and 37.5 % AC yielded a base NH_4^+ mass difference of 1.8 g-NH_4^+, whereas the feed of 37.5 % AC compared to 100 % AC resulted in a difference of 0.8 g-NH_4^+. Results indicated that beyond 37.5 % AC, a further increase in the proportion AC had a marginal effect on NH_4^+ recovery in the base. The total NH_4^+ mass balance (NH_4^+ in the diluate, base, and acid compartments) showed a recovery of 90 ± 3 %. The observed loss likely resulted from periodic sampling (every 15 min) and residual solution retained in the tubing and membrane stack, even though measures were taken to minimize it.

The NH_4^+ recovery efficiency (Fig. 2B) after an experimental run of 135 min was 26.8 % for 0 % AC feed, 38.6 % for 37.5 % AC and 45.2 % for 100 % AC, calculated using eq. (1). Comparable NH_4^+ recovery efficiency trends to those reported by Mutahi et al. [16] were observed for pure AS and pure AC. However, the NH_4^+ recovery efficiencies obtained in this study were lower than those reported by Mutahi et al. [16], who found values of 27.8 % for pure AS and 60.1 % for pure AC. Observed differences might be attributable to differences in the types of the membranes used, cell arrangement, initial NH_4^+ concentration in the feed, and experimental duration. Ammonia volatilization from the base compartment may also have contributed to the lower NH_4^+ recovery efficiencies, particularly since the base pH was sufficiently high to promote the NH_3(aq)-NH_3(g) equilibrium. Notably, the final pH of the base after an experimental run of 135 min ranged between 11.0 for pure AS and 12.3 for pure AC. The lower NH_4^+ removal from the diluate and reduced NH_4^+ recovery efficiency in the base with AC-poor/AS-rich feed mixtures can be attributed to strong competition between H^+ and NH_4^+ for transport across the CEM [10,14]. As shown in Fig. 5A, the pH of 100 % AS feed decreased from pH 7.3 to pH 3 within the first ten minutes of the experiment, whereas for feed mixture AS 87.5 % - AC 12.5 %, this took 40 min, indicating a higher concentration of H^+ in the diluate with increasing concentration of AS (Fig. 5B). The differences in H^+ leakages between AS and AC feed mixtures are further discussed in Section 3.3.

At elevated pH, uncharged dissolved NH_3 can diffuse through ion-exchange membranes (IEMs) and BPMs [10,24]– [26]. In this study, 30–40 % of the NH_4^+ transported from the feed to the base accumulated in the acid compartment via NH_3 diffusion from the base through the BPMs, consistent with our previous work [10]. Ion chromatographic analysis showed that after an experimental run of 135 min no NH_4^+ accumulation was detected in the electrode rinse solution. This observation was attributed to the use of AEEMs in the BPMED membrane stack, consistent with previous studies [10,12].

3.2. NH_4^+ current efficiency and energy consumption

Fig. 3A shows the NH_4^+ current efficiency, whereas Fig. 3B shows the energy consumption for different AS-AC feed mixtures. A lower % AC in the feed, for instance, 0 % AC feed compared to 100 % AC, resulted in a lower NH_4^+ current efficiency (20.4 % compared to 34.8 %) and higher energy consumption (22.3 kWh/kg-N recovered compared to 14.1 kWh/kg-N recovered). This trend was attributed to reduced NH_4^+ recovery in

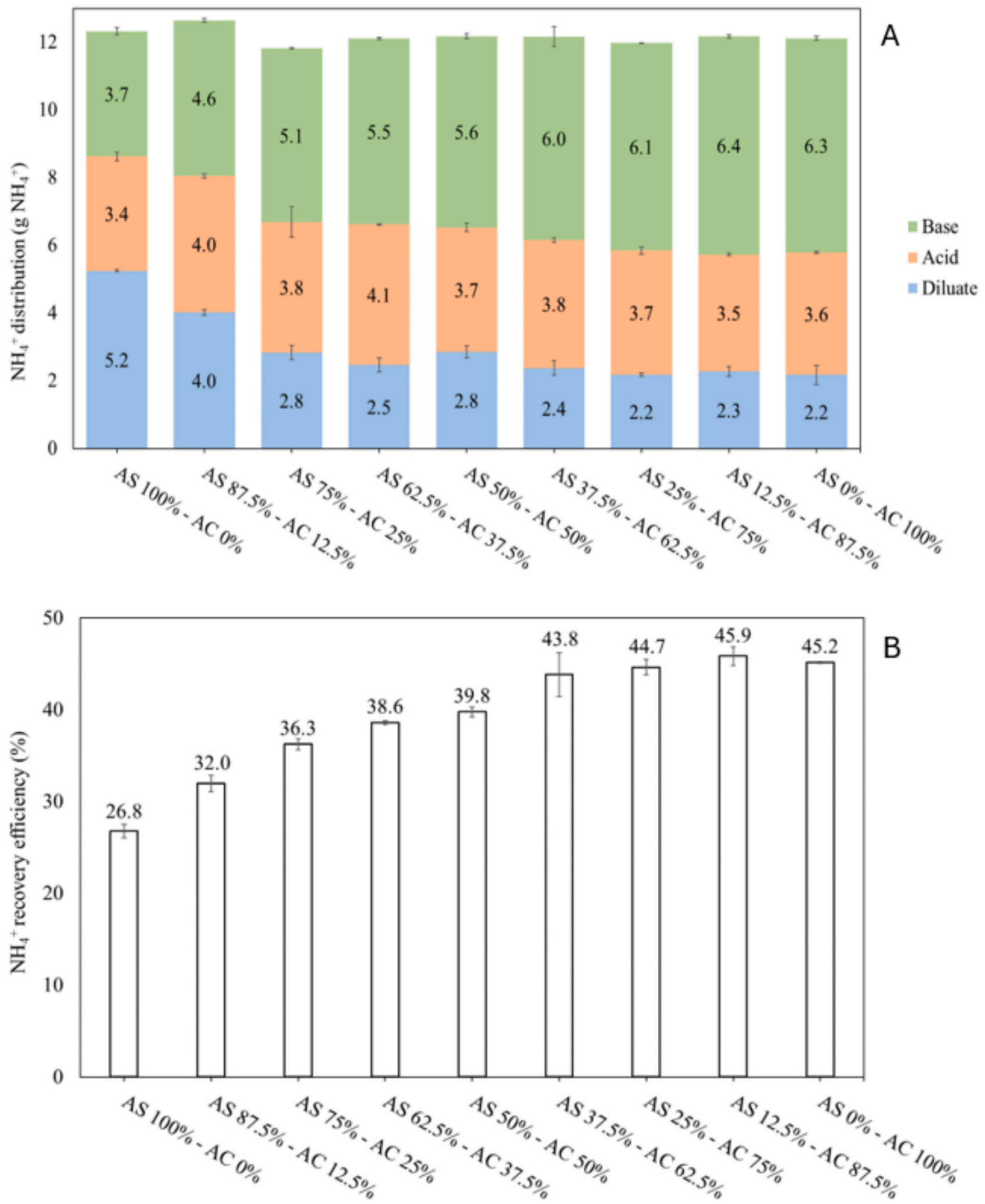

Fig. 2. Ammonium distribution over the diluate, acid, and base compartments (A) and ammonium recovery efficiency (B) after an experimental run of 135 min, resulting from ammonium sulfate (AS) and ammonium citrate (AC) feed mixtures in different proportions. All experiments were conducted with an initial NH_4^+ concentration of 0.757 ± 0.005 mol/L (13.6 ± 0.1 g NH_4^+ /L) and an initial pH of 7.3 ± 0.1, at a temperature of 25 ± 2 °C. Average values of the triplicate experiments are presented, along with the error bars.

the base compartment (3.7 g-NH_4^+ with 0 % AC feed compared to 6.3 g-NH_4^+ with 100 % AC feed), resulting from competitive ion transport at low pH (see Section 3.1).

The loss in NH_4^+ current efficiency due to diffusion of NH_3 from the base to the acid compartment was 19–23 %. Other possible causes for the loss in NH_4^+ current efficiency in this study are NH_3 diffusion and OH^- leakage from the base to the diluate compartment through the CEM [12,16,26]. OH^- is susceptible to leakage through CEMs primarily due to their small ionic radius and high mobility, which reduces the effectiveness of CEMs in excluding anions despite their intended cation-selective function [1]. In this study, OH^- leakage was inferred from the gradual pH increase observed in the diluate compartment, particularly in AC-rich feed mixtures (Fig. 5A). The differences in OH^- leakage between AS-AC mixtures are further discussed in Section 3.3.

To assess the influence of electrical resistance of the BPMED stack on energy consumption, the electrical conductivity (EC) of the feed solutions and the electric potential across the BPMED stack were analyzed. A high EC generally corresponds to low electric potential across the stack, reducing electrical resistance and energy consumption [12,27,28]. However, the EC differences in the feed solutions (Fig. 4A), only showed limited effects on the electric potential across the BPMED stack (Fig. 4B). Results indicated a limited impact of BPMED stack resistance on energy consumption, consistent with the findings of Mutahi et al. [16].

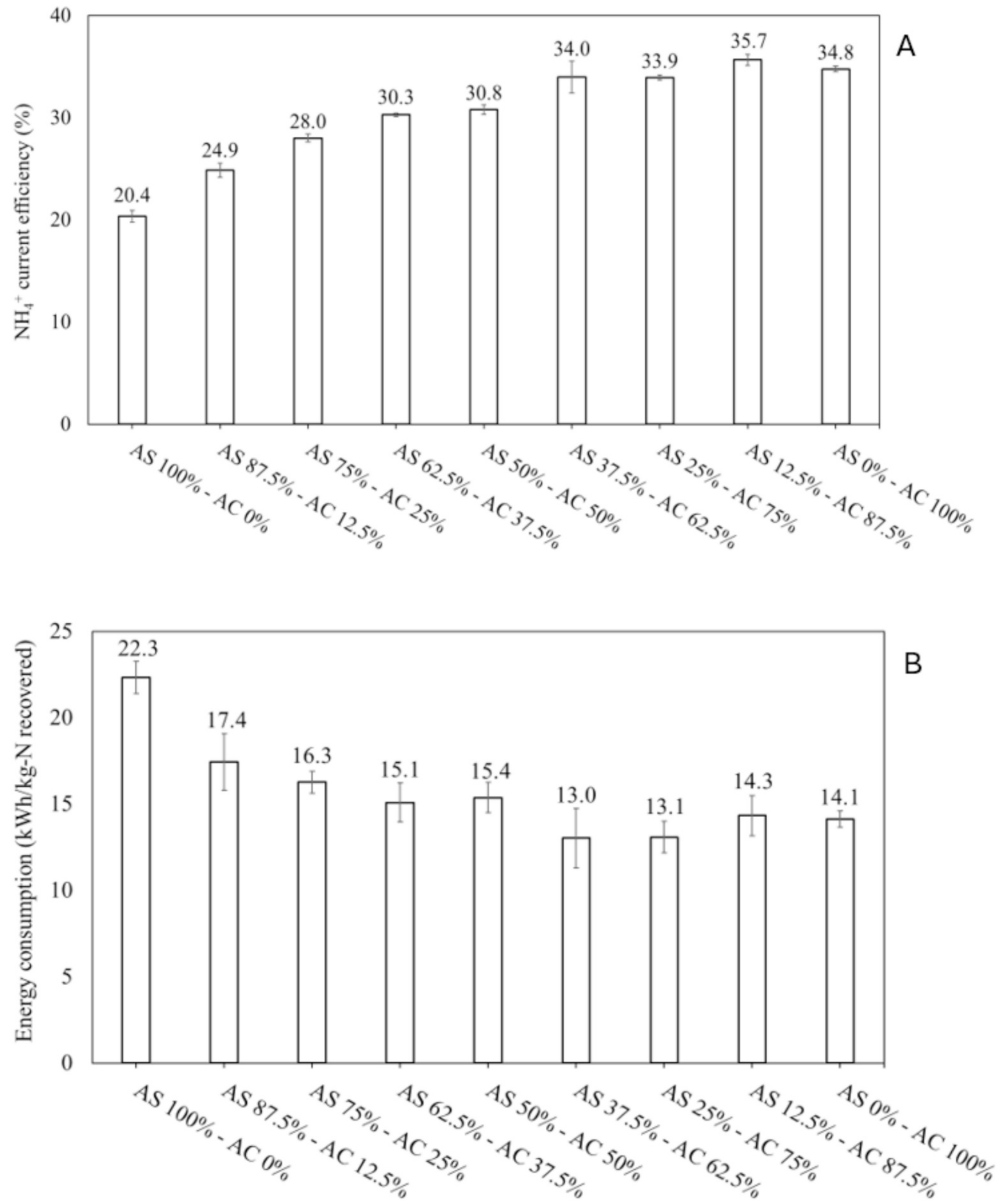

Fig. 3. Ammonium current efficiency (A) and energy consumption (B) with different ammonium sulfate (AS) and ammonium citrate (AC) feed mixtures proportions. All experiments were conducted with an initial NH_4^+ concentration of 0.757 ± 0.005 mol/L (13.6 ± 0.1 g NH_4^+/L), initial pH of 7.3 ± 0.1 and at a temperature of 25 ± 2 °C. Average values of the triplicate experiments are presented, along with the error bars.

3.3. H^+ and OH^- leakages to the diluate

In this study, an initial pH of 7.3 was selected for all feed solutions. Fig. 5A shows the pH evolution in the diluate over time, while Fig. 5B shows the corresponding H^+ concentration, directly calculated from the pH measurements. Feed solution with a higher or equal proportion of AS, i.e., AS 100 % - AC 0 % up to AS 50 % - AC 50 % resulted in an acidic diluate, whereas those with a higher proportion of AC led to a basic diluate. For AS-rich mixtures, H^+ leakage from the acid to the diluate compartment dominated over OH^- leakage from the base. Any potential OH^- leakage was likely neutralized by available H^+ in the diluate, explaining its acidic nature. The rapid decrease in diluate pH observed for the pure AS feed, from 7.3 to 3.0 within the first 10 min, can be attributed to substantial H^+ leakage from the acid compartment, indicating limited selectivity of the AEM for multivalent anions over protons under these initial experimental conditions. In contrast, AC is a salt of a weak polyprotic organic acid with multiple pKa values (2.9, 4.4, 5.7, 13.5) (Fig. 6) [29]. Based on the first three pKa values of citric acid ($pKa_1 = 2.9$, $pKa_2 = 4.4$, $pKa_3 = 5.7$) [29], the dominant citrate species in the experimental pH range (6.5–8.0) are $HCit^{2-}$ and Cit^{3-}, with Cit^{3-} becoming increasingly prevalent at higher pH. The higher negative charge of Cit^{3-} strengthens its electrostatic attraction to the positively charged sites of the anion exchange membrane (AEM), promoting its transport across the membrane. Conversely, under lower pH conditions, the presence of the less charged species H_2Cit^- reduces this interaction, leading to lower anion migration. AC-rich solutions exhibited distinct pH profiles due to the buffering capacity of citrate. Citrate ions neutralized H^+ leakage from the acid compartment, allowing OH^- leakage from the base to increase the diluate pH. After an experimental run of 135 min, the final pH of the acid varied between 1.2 for pure AS and 3.0 for pure AC, meaning that it can be reused as a scrubbing solution. In contrast, the final pH of the base varied between 11.0 for pure AS and 12.3 for pure AC.

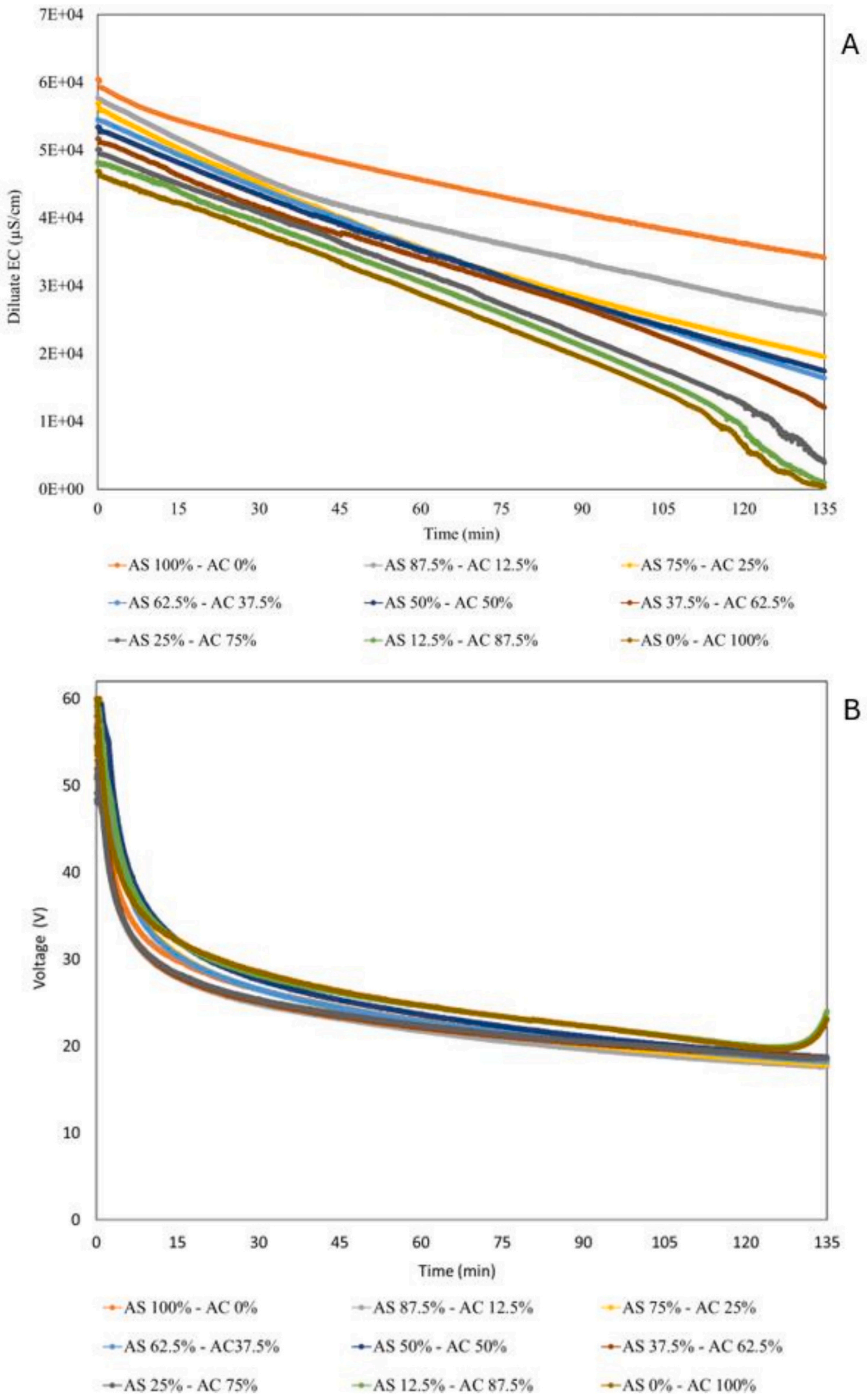

Fig. 4. Electrical Conductivity (EC) of the diluate (A) and electric potential across the BPMED membrane stack (B) during all experimental runs with different ammonium sulfate (AS) and ammonium citrate (AC) feed mixtures proportions. All experiments were conducted with an initial NH_4^+ concentration of 0.757 ± 0.005 mol/L (13.6 ± 0.1 g NH_4^+/L), initial pH of 7.3 ± 0.1 and at a temperature of 25 ± 2 °C.

3.4. Assessment of the anions mass balance and transport across anion exchange membranes (AEMs)

Fig. 7 shows the removal efficiencies of sulfate and citrate for different AS and AC feed mixtures, as calculated using Eq. 5. Relatively high SO_4^{2-} removal efficiency was observed for feed mixtures with low initial SO_4^{2-} concentration, whereas low citrate removal efficiency was associated with low initial citrate concentration. For instance, feed mixture AS 12.5 % - AC 87.5 % (initial SO_4^{2-} concentration of 0.044 mol/L) exhibited SO_4^{2-} removal efficiency of 95.1 %, whereas feed mixture AS 87.5 % - AC 12.5 % (initial citrate concentration of 0.034 mol/L) resulted in citrate removal efficiency of 29.1 %. These results confirm

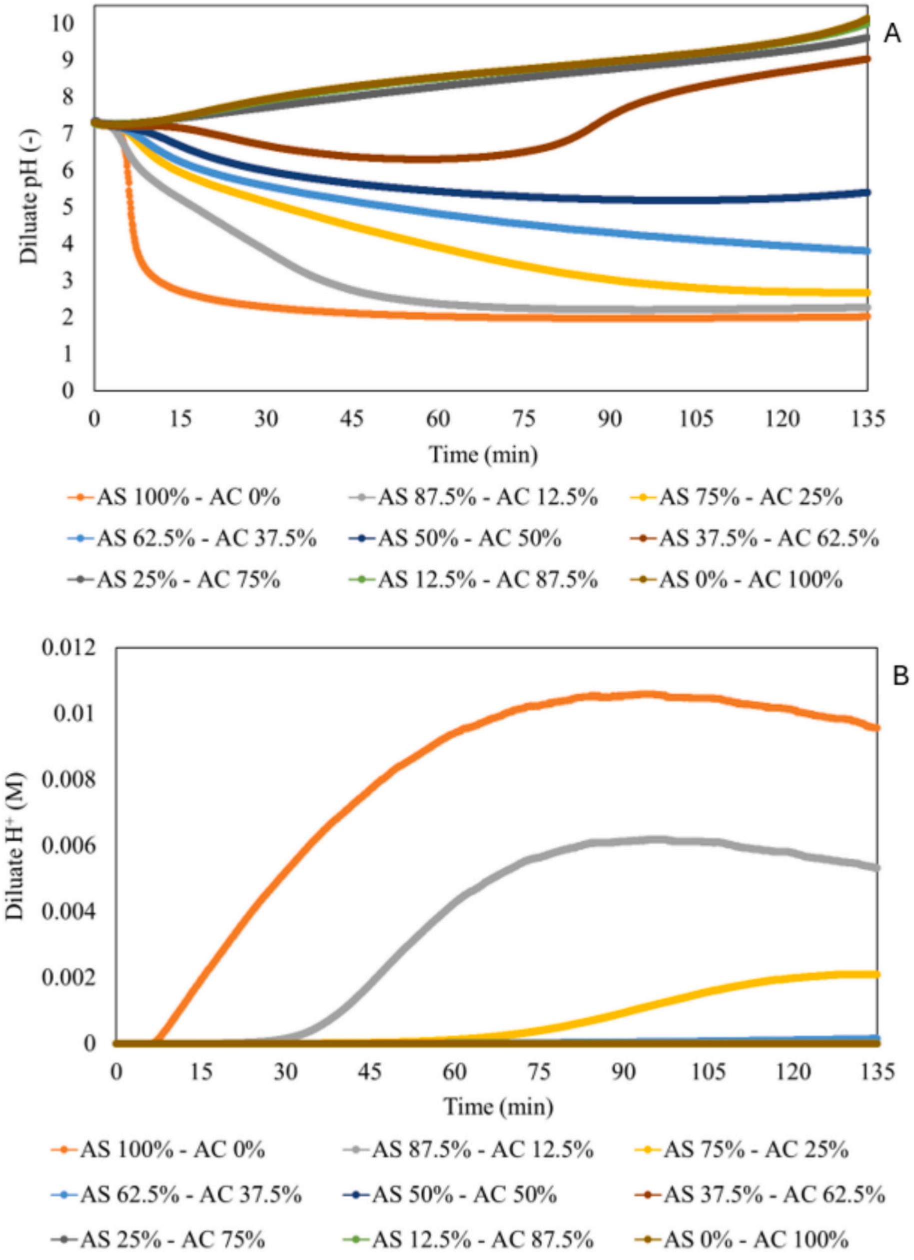

Fig. 5. Diluate pH over time (A) and concentration of H^+ in the diluate over time (B) throughout the experimental runs with different proportions of ammonium sulfate (AS) and ammonium citrate (AC) in the feed. All experiments were conducted with an initial NH_4^+ concentration of 0.757 ± 0.005 mol/L (13.6 ± 0.1 g NH_4^+/L), initial pH of 7.3 ± 0.1 and a temperature of 25 ± 2 °C.

that SO_4^{2-} transport was favored over citrate across AEMs, likely due to its higher mobility (Table 3), consistent with the study of Shi et al. [30].

In the membrane phase, competitive ion transport through the AEM likely occurred between sulfate species (HSO_4^- and SO_4^{2-}) and citrate species (H_2Cit^-, $HCit^{2-}$ and Cit^{3-}). Both anions are multivalent and interact strongly with the positively charged functional groups of the AEM. Under similar ionic strength conditions, Cit^{3-} exhibits a higher charge density and therefore a stronger electrostatic attraction to the membrane, which can enhance its transport relative to SO_4^{2-}. However, the larger molecular size and more complex structure of citrate impose steric limitations that partially restrict its mobility through the membrane matrix. Consequently, overall anion transport is governed by a balance between electrostatic affinity and steric hindrance effects, influencing charge balance and ion selectivity in AC-rich mixtures.

Feed solutions with a high AC fraction, i.e., AS 0 % - AC 100 % compared to AS 87.5 % - AC 12.5 %, showed increased citrate removal efficiency: 96.6 % compared to 29.1 %, respectively. As shown in Fig. 6, citrate dissociates fully at pH >8, existing predominantly as citrate (Cit^{3-}), whereas hydrogen citrate ($HCit^{2-}$) and dihydrogen citrate (H_2Cit^-) are more prevalent in acidic solutions. Fig. 5A shows that AC-rich feed solutions resulted in a basic diluate, favoring the presence of Cit^{3-}. With a mobility 1.3× and 2.3× higher than $HCit^{2-}$ and H_2Cit^-, respectively (Table 3), very likely Cit^{3-} exhibited enhanced transport.

Furthermore, the SO_4^{2-} and citrate mass balance across the diluate, acid, and base compartments was also calculated using eq. (6); results are shown in Fig. 8. A negative or positive anion mass balance after an experimental run time t either indicates anion mass loss or anion mass increase, with respect to the initial mass of anions. A negative SO_4^{2-} mass balance was observed for AS 100 % - AC 0 % (−3.0 g) to AS 62.5 % - AC 37.5 % (−1.1 g), indicating electromigration of sulfate to the ERS. In contrast, a positive balance was observed for AS 37.5 % - AC 62.5 % (2.1 g) to AS 0 % - AC 100 % (5.5 g), indicating electromigration of sulfate

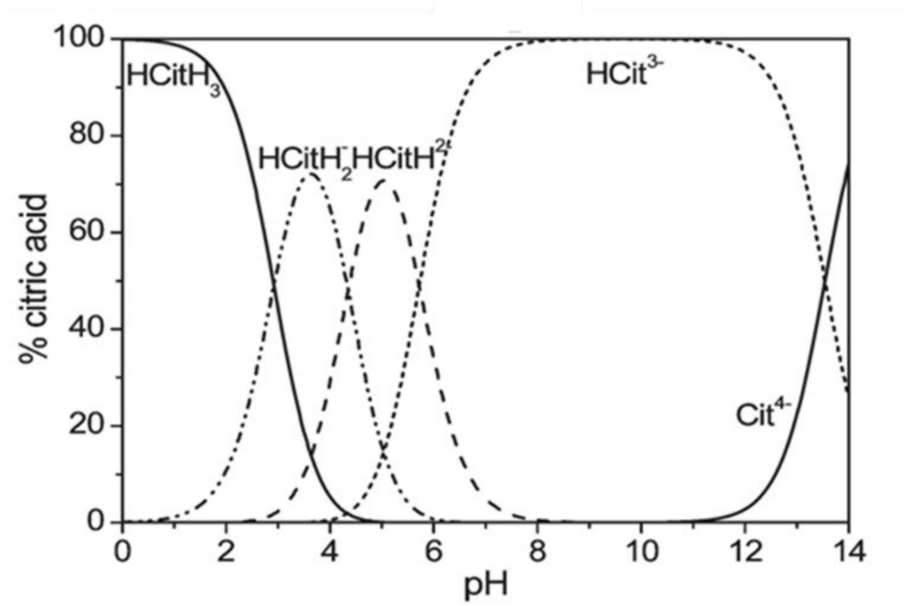

Fig. 6. pH-dependent deprotonation profile of citric acid. Citric acid undergoes stepwise deprotonation according to its four pKa values: 2.9, 4.4, 5.7, and 13.5 [29], corresponding to the sequential loss of its three carboxylic protons and one hydroxyl proton at high pH.

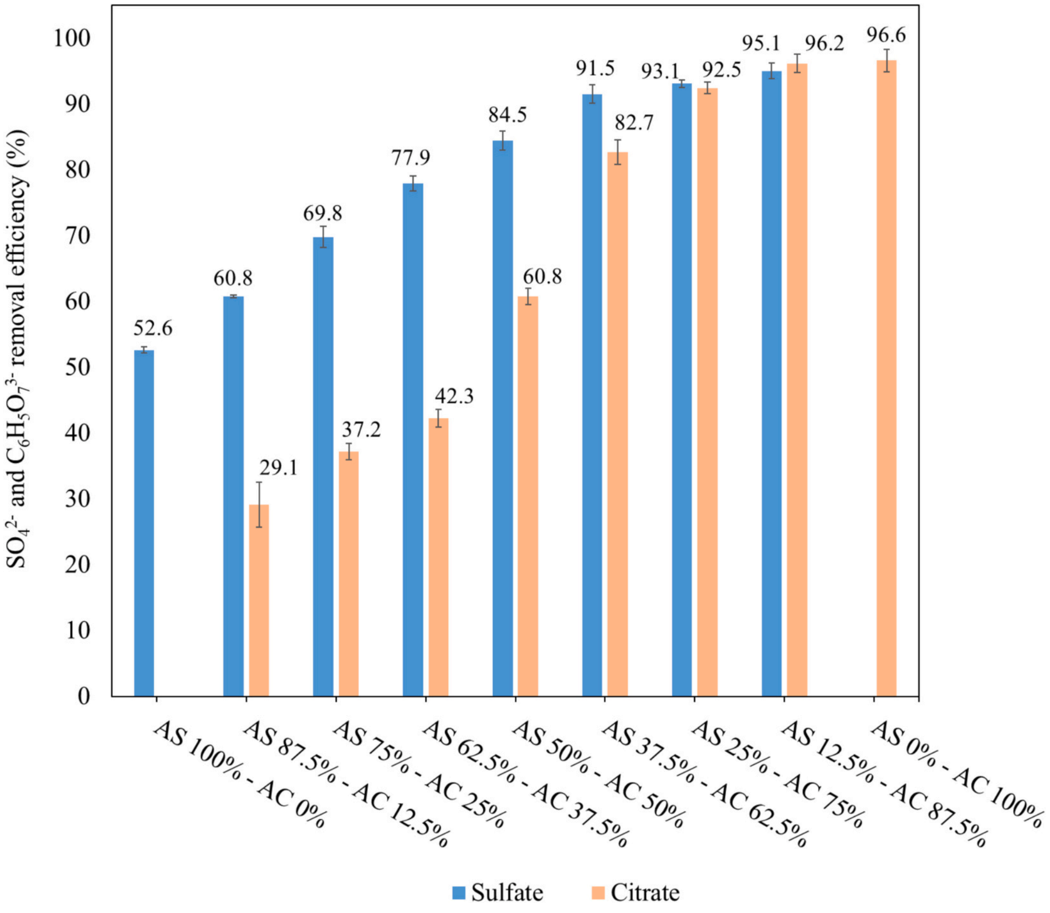

Fig. 7. Anions (sulfate and citrate) removal efficiency after an experimental period of 135 min, resulting from ammonium sulfate (AS) and ammonium citrate (AC) feed mixtures in different proportions. All experiments were conducted with an initial NH_4^+ concentration of 0.757 ± 0.005 mol/L (13.6 ± 0.1 g NH_4^+/L), initial pH of 7.3 ± 0.1 and at a temperature of 25 ± 2 °C. Average values of the triplicate experiments are presented, along with the error bars.

Table 3
Diffusion coefficient [31–33] and mobility of sulfate and citrate (calculated using eq. (7)).

Anion	Diffusion coefficient (m^2/s)	Mobility ($m^2\ V^{-1}\ s^{-1}$)
SO_4^{2-}	$1.07\cdot10^{-9}$	$8.33\cdot10^{-8}$
Cit^{3-}	$6.23\cdot10^{-10}$	$7.28\cdot10^{-8}$
$HCit^{2-}$	$7.11\cdot10^{-10}$	$5.54\cdot10^{-8}$
H_2Cit^-	$7.99\cdot10^{-10}$	$3.11\cdot10^{-8}$

from the concentrated Na_2SO_4 ERS to the acid compartment. The AS 50 % - AC 50 % mixture yielded a well-fitted sulfate mass balance (0 %). Similarly, AC-rich solutions, i.e., AS 0 % - AC 100 % compared to AS 87.5 % - AC 12.5 %, resulted in a more negative citrate mass balance: −7.8 g compared to −0.2 g, respectively. This observation can be attributed to the electromigration of citrate to the ERS. This observation is consistent with the observed positive SO_4^{2-} mass balance with AC-rich solutions, resulting from the electromigration of sulfate from the concentrated Na_2SO_4 ERS to the acid compartment (see the cell configuration in Fig. 1). Electromigration to and from the ERS maintained charge balance in the electrochemical cell. Notably, citrate losses primarily occurred via migration from the diluate to the anode ERS, with negligible return through the cathode (see the cell configuration in Fig. 1), as indicated by the absence of a positive citrate balance in this study (see Fig. 8). The composition of the ERS is therefore likely to vary depending on the feed mixture composition. Some mass loss in both SO_4^{2-} and citrate likely resulted from periodic sampling (every 15 min) and residual solution retained in tubing and the membrane stack, despite efforts to minimize those losses. Notably, SO_4^{2-} and citrate leakage from the acid and diluate compartments into the base was limited, ranging between 0.5 % - 3.5 % of their initial feed masses. The charge balance adjustments observed during BPMED operation resulted from both cation migration and co-ion leakage. In AS-rich mixtures, charge transfer was dominated by NH_4^+ migration and H^+ leakage from the acid compartment, leading to a more acidic diluate. In contrast, in AC-rich mixtures, the buffering capacity of citrate neutralized leaked H^+, while OH^- back diffusion through the CEM resulted in a slight pH increase. The presence of highly charged Cit^{3-} anions further promoted their transport across the AEM, contributing to the overall charge balance.

Notably, the diffusion coefficient values for $HCit^{2-}$ are not available in literature. Therefore, a reasonable estimate was obtained by averaging the diffusion coefficients of Cit^{3-} and H_2Cit^-, which was then used to calculate the mobility of $HCit^{2-}$.

3.5. *Overall discussion and future outlook*

This study comprehensively evaluated the effect of NH_4^+ salts mixtures (ammonium sulfate and ammonium citrate) on the NH_4^+ recovery efficiency, NH_4^+ current efficiency, energy consumption, NH_3 diffusion, H^+ and OH^- leakage to the diluate compartment, and anions transport across anion exchange membranes (AEMs) during BPMED. The results highlighted strong influence of feed solution mixtures, membrane transport mechanisms, and overall system performance.

The progressive increase in NH_4^+ recovery efficiencies in the base compartment with increasing AC proportion highlighted the role of the feed composition in enhancing NH_4^+ transport efficiency. Pure AC feed yielded the highest NH_4^+ recovery efficiency, whereas pure AS feed resulted in substantial NH_4^+ retention in the diluate. The buffering capacity of citrate, as a polyprotic acid, played a central role in mitigating H^+ accumulation in the diluate, with H^+ concentrations of $7.1\cdot10^{-11}$ $mol.L^{-1}$ for pure AC and $9.6\cdot10^{-3}$ $mol.L^{-1}$ for pure AS after an

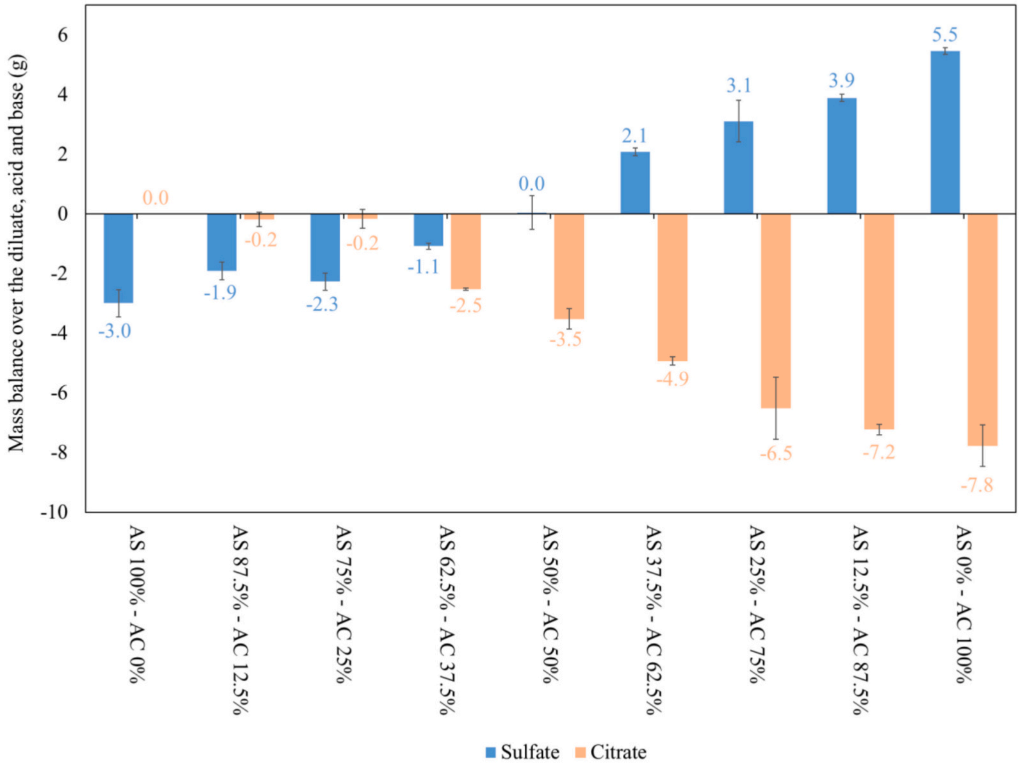

Fig. 8. Sulfate and citrate mass balance over the diluate, acid and base compartment after an experimental period of 135 min, resulting from ammonium sulfate (AS) and ammonium citrate (AC) feed mixtures in different proportions. A negative anion mass balance indicates a loss relative to the initial anion mass, while a positive balance signifies an excess. All experiments were conducted with an initial NH_4^+ concentration of 0.757 ± 0.005 mol/L (13.6 ± 0.1 g NH_4^+/L), initial pH of 7.3 ± 0.1 and at a temperature of 25 ± 2 °C. Average values of the triplicate experiments are presented, along with the error bars.

experimental run of 135 min, corresponding to a difference of 1.4×10^8. The AC buffering capacity maintained favorable pH conditions for NH_4^+ transport to the base compartment.These findings were consistent with competitive ion transport mechanisms described in literature, where high concentrations of H^+ at low pH hinders NH_4^+ transport across cation exchange membranes (CEMs) [10,14]. Additionally, NH_3 diffusion from the base to the acid, along with possible NH_3 volatilization at elevated pH, contributed to losses in NH_4^+ recovery and current efficiency, emphasizing the importance of controlling uncharged species transport in BPMED applications [23,25].

Higher NH_4^+ recovery with AC-rich feeds led to lower energy consumption, although the electrical resistance of the BPMED stack had only a limited influence, as variations in feed EC did not result in substantial changes in electric potential. This indicated that voltage losses were primarily governed by ion transport limitations rather than ohmic resistance and that ion transport mechanisms, including H^+ and OH^- leakage, had a greater impact on energy performance than stack resistance, consistent with findings reported in previous studies [16]. OH^- leakage, as indicated by the pH increase of the diluate with particularly the AC-rich feeds used in this study, reflected the known selectivity limitations of CEMs [1]. Table 4 presents a comparison of NH_4^+ recovery efficiency, NH_4^+ current efficiency, and energy consumption between this study and that of Mutahi et al. [16]. The observed differences are possibly due to the types of membranes used, the cell arrangement, the initial NH_4^+ concentration in the feed, and the experimental duration.

In addition, the NH_4^+ current efficiency increased with increasing AC proportion, reflecting reduced competitive ion interference and enhanced transmembrane transport. However, NH_4^+ losses resulting from NH_3 diffusion, possible NH_3 volatilization at elevated pH, and OH^- leakage through the CEM, contributed to lower-than-optimal current efficiencies, thereby reducing NH_4^+ recovery efficiency and increasing energy consumption. To improve process performance, future studies and system designs should focus on mitigating NH_3 diffusion and OH^- leakage. Membrane modification, such as reducing CEM porosity may reduce OH^- leakage. Operating at a lower pH in the base compartment can reduce NH_3 volatilization [34] and may therefore limit subsequent NH_3 diffusion to the acid compartment. Additionally, system configuration changes, such as reducing intermembrane spacing, optimizing flow rate and current operation through pulse-pause regimes, or applying vacuum membrane stripping (VMS) to rapidly extract NH_3 from the base, can decrease the residence time of NH_3 in the system and reduce co-ion transport [34–36]. Implementing these measures may enhance overall NH_4^+ recovery efficiency and reduce energy consumption.

The findings of this study clearly indicated that feed mixtures containing as little as 37.5 % AC already significantly enhanced system performance with respect to NH_4^+ recovery efficiency, current efficiency and energy consumption, potentially contributing to overall cost savings. Increasing the AC proportion beyond 37.5 % resulted in only marginal improvements in NH_4^+ recovery efficiency, and reduced energy consumption and NH_3 diffusion from the base to the acid compartment. This suggested the presence of a threshold beyond which additional AC yields progressively smaller benefit, likely due to the saturation of beneficial effects such as buffering capacity and reduced H^+ competition.

Table 4
Comparison of NH_4^+ recovery efficiency, NH_4^+ current efficiency, and energy consumption between this study and Mutahi et al. [16].

Study	Feed Composition	NH_4^+ Recovery Efficiency (%)	NH_4^+ Current Efficiency (%)	Energy Consumption (kWh/kg-N)
This study	AS	26.8	20.4	22.3
	AS - AC mixtures	32.0–45.9	24.9–35.7	13.0–17.4
	AC	45.2	34.8	14.1
Mutahi et al. [16]	AS	27.8	21.5	15.6
	AC	60.1	46.5	7.2

Furthermore, AC-rich feeds exhibited increased citrate removal efficiency, due to the formation of the highly mobile Cit^{3-} species at elevated pH in the diluate. Anion transport assessment indicated that SO_4^{2-} transport was favored over citrate across AEMs, likely due to its higher mobility.

Finally, these results highlighted the importance of optimizing feed composition, not only regarding the choice of ammonium salt but also the buffering capacity of the anion-acid pair in order to achieve a balanced performance across ion transport, NH_4^+ recovery and energy consumption. AC-rich feeds offered clear benefits, including enhanced NH_4^+ recovery efficiency and improved pH stability for NH_4^+ transport. However, they also introduced challenges such as more complex anion transport behavior and potential losses to unintended compartments. In addition, it is important to acknowledge certain experimental limitations in this study. Synthetic feed solutions were used rather than actual scrubber effluents, which may differ in composition and buffer capacity. Minor pH drift over time could have affected ion transport dynamics, and potential gas-phase NH_3 losses may have influenced NH_4^+ recovery efficiency and energy consumption. These factors should be considered when extrapolating the findings to upscaled applications. Future system designs should consider strategies such as targeted pH control, enhanced membrane selectivity, improved configuration and suitable pretreatment approaches to minimize undesired ion leakage and improve overall process efficiency.

4. Conclusions

This study investigated the effect of varying ammonium citrate – ammonium sulfate proportional mixtures on NH_4^+ recovery efficiency, NH_4^+ current efficiency, energy consumption, NH_3 diffusion from the base to the acid compartment, H^+ and OH^- leakage to the diluate compartment, and anion transport across AEMs during BPMED. The NH_4^+ recovery efficiency was higher, and energy consumption lower, for pure ammonium citrate (45.2 %, 14.1 kWh/kg-N) and mixture solutions (32.0–45.9 %, 13.0–17.4 kWh/kg-N) compared to pure ammonium sulfate (26.8 %, 22.3 kWh/kg-N). These improvements were can be attributed to reduced ion competition between H^+ and NH_4^+ for transport across the CEM, as supported by the observed pH trends in the diluate. The NH_4^+ current efficiency was higher for pure ammonium citrate (34.8 %) and mixture solutions (24.9–35.7 %) compared to pure ammonium sulfate solution (20.4 %). Losses in NH_4^+ current efficiency were attributed, among other factors, to H^+ transport across the CEM and NH_3 diffusion from the base to the acid compartment. NH_3 diffusion caused a 19–23 % loss in NH_4^+ current efficiency, accounting for a 30–40 % of the NH_4^+ transported from the feed. The enhanced NH_4^+ recovery and current efficiency observed in ammonium citrate-rich feeds can be attributed to the combined effects of chemical buffering and electromigration. Feed mixtures with a higher proportion of ammonium citrate than ammonium sulfate functioned as effective chemical buffers, neutralizing H^+ ions that would otherwise leak from the acid to the diluate compartment and thereby maintaining favorable pH conditions for NH_4^+ transport. In addition to this buffering effect, electromigration under the applied electric field governed the transport of ions, including NH_4^+, SO_4^{2-} and citrate species, with SO_4^{2-} transport favored over citrate species across the AEMs due to its higher mobility. Ammonium citrate-rich mixtures also exhibited higher citrate removal efficiencies, due to the higher mobility of Cit^{3-} compared to $HCit^{2-}$ and H_2Cit^-, as well as the increased citrate concentration gradient between the diluate and acid compartments. Although BPMED of simulated scrubber effluents containing NH_4^+ salts mixtures of ammonium sulfate and ammonium citrate demonstrated the feasibility of achieving high NH_4^+ recovery efficiency and current efficiency with low energy consumption, further experiments with real scrubber effluents are necessary to evaluate the impact of additional ions and membrane fouling on process performance, assess long-term operation, and assess the overall techno-economic feasibility of the BPMED system.

CRediT authorship contribution statement

Dhavissen Narayen: Writing – original draft, Visualization, Validation, Methodology, Investigation, Formal analysis, Data curation, Conceptualization. **Elif Başli:** Methodology, Investigation, Formal analysis. **Jules B.van Lier:** Writing – review & editing, Supervision. **Henri Spanjers:** Writing – review & editing, Supervision.

Declaration of competing interest

The authors declare that they have no known competing financial interests or personal relationships that could have appeared to influence the work reported in this paper.

Acknowledgments

This work was supported by the Netherlands Enterprise Agency, also known as Rijksdienst voor Ondernemend Nederland (RVO) [Project No. TEHE119005]. This study was performed within the “Kostprijsreductie bioenergie door Chemical Free Ammonium Recovery” (NoChemNAR) research. We would like to acknowledge the contribution of David A. Vermaas for his guidance and help during the research. We would like to acknowledge the staff from TU Delft Waterlab, especially Armand Middeldorp for his support in the laboratory.

Data availability

Data will be made available on request.

References

[1] H. Strathmann, Electrodialysis, a mature technology with a multitude of new applications, Desalination 264 (3) (2010) 268–288, https://doi.org/10.1016/j.desal.2010.04.069.

[2] H. Strathmann, Ion-exchange membrane separation processes, 2004.

[3] W. Chen, S. Grimberg, S. Rogers, T. Kim, Bipolar membrane electrodialysis for nutrient recovery from anaerobic digestion dewatering sidestream, Chem. Eng. J. 488 (2024) 150834, https://doi.org/10.1016/j.cej.2024.150834.

[4] F. Ferrari, M. Pijuan, S. Molenaar, N. Duinslaeger, T. Sleutels, P. Kuntke, J. Radjenovic, Ammonia recovery from anaerobic digester centrate using onsite pilot scale bipolar membrane electrodialysis coupled to membrane stripping, Water Res. 218 (2022) 118504, https://doi.org/10.1016/j.watres.2022.118504.

[5] X. Guo, J. Chen, X. Wang, Y. Li, Y. Liu, B. Jiang, Sustainable ammonia recovery from low strength wastewater by the integrated ion exchange and bipolar membrane electrodialysis with membrane contactor system, Sep. Purif. Technol. 305 (2023), https://doi.org/10.1016/j.seppur.2022.122429.

[6] I. Kaniadakis, J.B. van Lier, H. Spanjers, Removal of total ammoniacal nitrogen from reject water through selective electrodialysis reversal and bipolar electrodialysis, Chem. Eng. J. 493 (2024) 152613, https://doi.org/10.1016/j.cej.2024.152613.

[7] J.K. Kim, H.G. Kim, L.K. Kwac, N. Jeong, K.S. Hwang, Improving ammonia nitrogen removal and recovery by BMED stack optimization: the effect of ion exchange membrane thickness, Chem. Eng. Sci. 296 (2024) 120203, https://doi.org/10.1016/j.ces.2024.120203.

[8] Y. Li, S. Shi, H. Cao, X. Wu, Z. Zhao, L. Wang, Bipolar membrane electrodialysis for generation of hydrochloric acid and ammonia from simulated ammonium chloride wastewater, Water Res. 89 (2016) 201–209, https://doi.org/10.1016/j.watres.2015.11.038.

[9] Y. Li, R. Wang, S. Shi, H. Cao, N.Y. Yip, S. Lin, Bipolar membrane Electrodialysis for Ammonia recovery from synthetic urine: experiments, modeling, and performance analysis, Environ. Sci. Technol. 55 (21) (2021) 14886–14896, https://doi.org/10.1021/acs.est.1c05316.

[10] D. Narayen, E. van Berlo, J.B. van Lier, H. Spanjers, Recovery of sulfuric acid and ammonia from scrubber effluents using bipolar membrane electrodialysis: effect of pH and temperature, Sep. Purif. Technol. 338 (2024) 126605, https://doi.org/10.1016/j.seppur.2024.126605.

[11] S. Panagoda, P. Yuan, V. Pavlovic, J. Barber, Y. Kim, Enhancing ammonia recovery through pH polarization in bipolar membrane electrodialysis, Environmental Science Advances 3 (9) (2024) 1309–1316, https://doi.org/10.1039/d4va00082j.

[12] N. van Linden, G.L. Bandinu, D.A. Vermaas, H. Spanjers, J.B. van Lier, Bipolar membrane electrodialysis for energetically competitive ammonium removal and dissolved ammonia production, J. Clean. Prod. 259 (2020) 120788, https://doi.org/10.1016/j.jclepro.2020.120788.

[13] M.A.B. Ali, M. Rakib, S. Laborie, P. Viers, G. Durand, Coupling of bipolar membrane electrodialysis and ammonia stripping for direct treatment of wastewaters containing ammonium nitrate, J. Membr. Sci. 244 (1) (2004) 89–96, https://doi.org/10.1016/j.memsci.2004.07.007.

[14] W. Guan, G. Zhang, L. Zeng, C. Zeng, G. Shang, A novel process on preparation of ammonium metatungstate solution using bipolar membrane electrodialysis, Can. Metall. Q. 56 (4) (2017) 432–441, https://doi.org/10.1080/00084433.2017.1363931.

[15] M. Rodrigues, S. Molenaar, J. Barbosa, T. Sleutels, H.V.M. Hamelers, C.J. N. Buisman, P. Kuntke, Effluent pH correlates with electrochemical nitrogen recovery efficiency at pilot scale operation, Sep. Purif. Technol. 306 (2023) 122602, https://doi.org/10.1016/j.seppur.2022.122602.

[16] G. Mutahi, J.B. van Lier, H. Spanjers, Leveraging organic acids in bipolar membrane electrodialysis (BPMED) can enhance ammonia recovery from scrubber effluents, Water Res. 265 (2024) 122296, https://doi.org/10.1016/j.watres.2024.122296.

[17] Z. Jamaludin, S. Rollings-Scattergood, K. Lutes, C. Vaneeckhaute, Evaluation of sustainable scrubbing agents for ammonia recovery from anaerobic digestate, Bioresour. Technol. 270 (2018) 596–602, https://doi.org/10.1016/j.biortech.2018.09.007.

[18] N. van Linden, H. Spanjers, J.B. van Lier, Fuelling a solid oxide fuel cell with ammonia recovered from water by vacuum membrane stripping, Chem. Eng. J. 428 (2022) 131081, https://doi.org/10.1016/j.cej.2021.131081.

[19] D. Wang, W. Meng, Y. Lei, C. Li, J. Cheng, W. Qu, G. Wang, M. Zhang, S. Li, The novel strategy for increasing the efficiency and yield of the bipolar membrane Electrodialysis by the double conjugate salts stress, Polymers 12 (2) (2020) 343, https://doi.org/10.3390/polym12020343.

[20] Y. Zhou, H. Yan, X. Wang, Y. Wang, T. Xu, A closed loop production of water insoluble organic acid using bipolar membranes electrodialysis (BMED), J. Membr. Sci. 520 (2016) 345–353, https://doi.org/10.1016/j.memsci.2016.08.011.

[21] P. Atkins, J. de Paula, Physical Chemistry, 11th ed., Oxford University Press, 2017.

[22] A.J. Bard, L.R. Faulkner, Electrochemical Methods: Fundamentals and Applications, 2nd ed., John Wiley & Sons, 2001.

[23] J.S. Jaime-Ferrer, E. Couallier, P. Viers, M. Rakib, Two-compartment bipolar membrane electrodialysis for splitting of sodium formate into formic acid and sodium hydroxide: modelling, J. Membr. Sci. 328 (1) (2009) 75–80, https://doi.org/10.1016/j.memsci.2008.10.058.

[24] R. Pärnamäe, S. Mareev, V. Nikonenko, S. Melnikov, N. Sheldeshov, V. Zabolotskii, H.V.M. Hamelers, M. Tedesco, Bipolar membranes: a review on principles, latest developments, and applications, J. Membr. Sci. 617 (2021) 118538, https://doi.org/10.1016/j.memsci.2020.118538.

[25] D. Saabas, J. Lee, Recovery of ammonia from simulated membrane contactor effluent using bipolar membrane electrodialysis, J. Membr. Sci. 644 (2022) 120081, https://doi.org/10.1016/j.memsci.2021.120081.

[26] A. Chandra, J.G.D. Tadimeti, S. Chattopadhyay, Transport hindrances with electrodialytic recovery of citric acid from solution of strong electrolytes, Chin. J. Chem. Eng. 26 (2) (2018) 278–292, https://doi.org/10.1016/j.cjche.2017.05.010.

[27] Y. Tanaka, Chapter six - Electrodialysis, in: S. Tarleton (Ed.), Progress in Filtration and Separation, Academic Press, Oxford, 2015, pp. 207–284, https://doi.org/10.1016/B978-0-12-384746-1.00006-9.

[28] H. Yan, Y. Wang, L. Wu, M.A. Shehzad, C. Jiang, R. Fu, Z. Liu, T. Xu, Multistage-batch electrodialysis to concentrate high-salinity solutions: process optimisation, water transport, and energy consumption, J. Membr. Sci. 570–571 (2019) 245–257, https://doi.org/10.1016/j.memsci.2018.10.008.

[29] A. Heller, A. Barkleit, H. Foerstendorf, S. Tsushima, K. Heim, G. Bernhard, Curium(iii) citrate speciation in biological systems: a europium(iii) assisted spectroscopic and quantum chemical study, Dalton Trans. 41 (45) (2012) 13969–13983, https://doi.org/10.1039/C2DT31480K.

[30] L. Shi, Y. Hu, S. Xie, G. Wu, Z. Hu, X. Zhan, Recovery of nutrients and volatile fatty acids from pig manure hydrolysate using two-stage bipolar membrane electrodialysis, Chem. Eng. J. 334 (2018) 134–142, https://doi.org/10.1016/j.cej.2017.10.010.

[31] J. Buffle, Z. Zhang, K. Startchev, Metal flux and dynamic speciation at (bio)interfaces. Part I: critical evaluation and compilation of physicochemical parameters for complexes with simple ligands and fulvic/humic substances, Environ. Sci. Technol. 41 (22) (2007) 7609–7620, https://doi.org/10.1021/es070702p.

[32] PhreeqC, A Computer Program for Speciation, Batch-Reaction, One-Dimensional Transport, and Inverse Geochemical Calculations; [The Diffusion Coefficients Are Taken From The Thermodynamic Database “phreeqc.dat”.]. (n.d.).

[33] P. Vanýsek, *Ionic Conductivity and Diffusion at Infinite Dilution, Handbook of Chemistry and Physics*, 1992/93 Ed, CRC Press, 1992.

[34] I. Kaniadakis, J.B. van Lier, H. Spanjers, Ammonia recovery in bipolar membrane electrodialysis via pH control through electric current pulse modulation, Water Res. 286 (2025) 124185, https://doi.org/10.1016/j.watres.2025.124185.

[35] S. Panagoda, P. Yuan, V. Pavlovic, J. Barber, Y. Kim, Enhancing ammonia recovery through pH polarization in bipolar membrane electrodialysis, Environ. Sci. Adv. 3 (9) (2024) 1309–1316, https://doi.org/10.1039/D4VA00082J.

[36] N. van Linden, Y. Wang, E. Sudhölter, H. Spanjers, J.B. van Lier, Selectivity of vacuum ammonia stripping using porous gas-permeable and dense pervaporation membranes under various hydraulic conditions and feed water compositions, J. Membr. Sci. 642 (2022) 120005, https://doi.org/10.1016/j.memsci.2021.120005.